

AUTOMATED LOCALISATION OF THE OPTIC DISC AND FOVEA TO ASSIST DIABETIC RETINOPATHY SCREENINGS

Hussain F Jaafar¹, Asoke K Nandi² and Waleed Al-Nuaimy³

¹Department of Electrical Engineering, Babylon University, Babylon, Iraq

²Department of Electronic and Computer Engineering, Brunel University, Uxbridge, UK

³Department of Electrical Engineering and Electronics, University of Liverpool, Liverpool, UK

¹hussain_engi@yahoo.com, ²asoke.nandi@brunel.ac.uk, ³wax@liverpool.ac.uk

ABSTRACT

The localisation of the anatomical structures in retinal fundus images is an important step in the automated analysis of retinal images. In this paper automated methods for the localisation of the optic disc and the fovea are proposed. For an optic disc localisation, the area of most vasculature loops is determined to locate an initial optic disc centre, followed by morphological operations and a circular Hough Transform to determine its boundary and the final centre. For fovea localization, foveal features and a model of geometric relations between the fovea and both the optic disc and the vasculature are used to locate its boundary and centre. Both methods were evaluated using two sets of images from different datasets, and their competitive performance indicate that they could be used for a computer-aided mass localisation of the optic disc and the fovea as part of an automatic screening programme.

Index Terms— Biomedical image processing, retinal vasculature, optic disc, fovea, morphological operations

1. INTRODUCTION

The optic disc (OD) is a spot on the retina where ganglion cells exit to form the optic nerves. It is also the entry point for the major vasculature that supplies the eye with blood. The fovea is the retinal part where the most of photoreceptor cells are concentrated; hence it is the most specialised part of the retina and responsible for all activities when visual detail are required.

Abnormalities associated with common eye diseases such as diabetic retinopathy are distributed non-uniformly over the retina [1]. The detection of abnormalities and knowing their spatial distributions with reference to the retinal anatomy, particularly the optic disc and the fovea, are very important steps in evaluating the presence and severity of diabetic retinopathy [2]. In addition, the location of the optic disc is an important issue in retinal image analysis because it is a significant landmark feature, and its diameter is used as a reference length for measuring distances and

sizes. Moreover, as the fovea is the centre of vision, the detection and diagnosis of lesions can provide a more precise and meaningful evaluation of the risk when the spatial locations are described with reference to the fovea location [3].

Fundus images are used for diagnosis by clinicians to check for abnormalities or any change in their features. Manual analysis and diagnosis of abnormalities in retinal images require a great deal of time and energy. Hence, computer-aided screening will save cost and time considering the large number of retinal images that need to be analysed.

The automated localisation of the optic disc and the fovea is a difficult task for images of variable quality and in the presence of abnormalities. Previous related works localised the OD using different methods, where some focused on intensity based features as in Lalonde *et al.* [4] and Reza *et al.* [5], who used the bright object features to distinguish the OD as the brightest region in the retinal image from the background. They tend to fail in OD localisation when the OD is not clear or there is an abnormality brighter than the OD. Other works used the fact that the OD is the region where the vasculature emerges and made use of the vasculature features in this region to localise the OD as in Foracchia *et al.* [6]. Other researchers made use of both facts that the OD is the brightest region and the origin of vasculature to localise it as in Sekhar *et al.* [7], and Fleming *et al.* [8].

For fovea localisation, some techniques used features of the fovea as being the darkest area, and the fovea centre location being below the OD centre as in Sinthanayothin *et al.* [9] and Welfer *et al.* [10]. In addition to the fovea features and location, its relative position with respect to the OD is used as in Fleming *et al.* [9]. Moreover, others used fovea features and its position with respect to the OD and the vasculature to localise the fovea as in Tobin *et al.* [11].

In this paper, a novel method for the OD localisation is proposed based on determination of the area of most vasculature loops and its centre is considered as an initial estimate of the OD centre. This is followed by boundary determination by computing the largest and the brightest

blobs of the image using adaptive histogram thresholding. With regard to the fovea localisation, a new method is presented based on the fovea features and geometric relations with the OD and main arcade of the vasculature.

This paper is structured as follows: Section 2 presents the methodology and outlines the main techniques used, Section 3 presents results and discussion, while conclusions are presented in Section 4.

2. METHODOLOGY

2.1. Optic Disc Localisation

In the literature, the majority of OD localisation techniques are based on OD features i.e. shape, size and colour. In some retinal images the OD is not clearly visible or some of bright lesions may look similar to the OD in shape, size and colour. In these cases, the techniques which are using OD features may fail to localise the OD.

In this paper, we propose a method based on the features of retinal vasculature and its spatial relation with the OD to localise the OD. The vessel map is turned into a network of vessels, branches, and loops, and then a network of most vasculature loops can be selected and used as candidate area for the initial OD centre.

- **Vasculature-loops.** A binary vasculature image is required to construct this network, where the vessels that are also connected in the original image should be connected in the binary image to accomplish a successful approach. To obtain an increase of vessel connectedness, an intervention on the threshold of the proposed vasculature detection is made to retrieve the entire vessels and ensure better vessel connectedness. Steps of determining the most vasculature loops are as follows:

1. *Increasing vasculature connectedness.* This is accomplished by decreasing the binarization threshold level used in the multi-scale technique for detection of the vasculature proposed in a previous work [12] by 5%. This operation increases true positives and retrieves entire vessels with some increase in the undesired false positives.
2. *Generating vessel skeleton.* A morphological skeletonisation is applied to the vasculature image. This operation largely preserves the extent and the connectivity of the original vessel while throwing away most of the foreground pixels.
3. *Removing small vessels.* The vessel is a group of many pixels where a small vessel starts with a pixel of one neighbour and ends with another pixel also of one neighbour. Small vessels are suppressed from the vasculature before classifying into loops and branches.
4. *Loop fitting.* The vessels inside the OD emerge and overlap forming loops and semi-loops in contrary to vessels outside the OD which are spread away from their origin. To fit small semi-loops in the vasculature image,

the method proposed by Qiao and Ong [13] was applied. In this fitting method, a connectivity-based algorithm for fitting multiple-circles is proposed, where false circle detection is solved using circular arcs, which are intra-connected subsets that agree with the circular models with a specified error.

5. *Suppressing large loops.* As the loops inside the OD are expected to be smaller than the OD, the original and fitted loops that have a major axis length bigger than a threshold (T) are excluded and considered as branch vessels, where T is the mean diameter of the OD which is found to be 16.5 times the average vasculature width according to what is found in [7].

- **Selection of most vasculature loops.** The most constructed vasculature loops can be used to find the initial OD centre. The OD contains the optic nerve from which a few main vessels split up into many smaller vessels which spread around the retina. Vasculature segments in this area of the retina are often small and are therefore often combined into several loops connected to each others. An increasing amount of vessel connections of a loop also increases the probability of the loop being located in the OD area. The procedure of determination of the initial OD centre is presented as follows:

1. The area of the most vasculature loops is selected as a candidate location for the OD.
2. The candidate OD location is surrounded by a boundary box where its centre is considered as initial OD centre.

Figure 1 illustrates results of allocating the most vasculature loops surrounded by a bounding box to determine the initial OD centre.

- **Boundary and final OD centre determination.** After localisation of the initial OD centre, boundary of the OD is determined by selecting a region of interest (ROI) within the area around an allocated initial OD centre. The selected ROI is a sub-image from a pre-processed green channel image with the same dimension proportion of the entire image and its smaller dimension is twice the mean diameter of the OD. Based on trial and error experiments carried out by [7] on images from different datasets, the OD mean diameter was found to be 16.5 times the average vasculature width for all datasets. Initial boundary of the OD is then determined by computing the largest and the brightest blobs within the sub-image using adaptive histogram thresholding method.

The magnitude gradient of the ROI is calculated using morphological operations. Initially, morphological closing is performed on the ROI to fill the vessels followed by morphological opening to remove large peaks. Then the gradient is calculated by subtracting the eroded ROI from the dilated one. A circular Hough Transform is applied to the reconstructed image to determine the boundary of the OD. The radius of the circular Hough Transform to find the optic disk boundary is calculated from the retinal vasculature width. After locating the OD boundary, the final

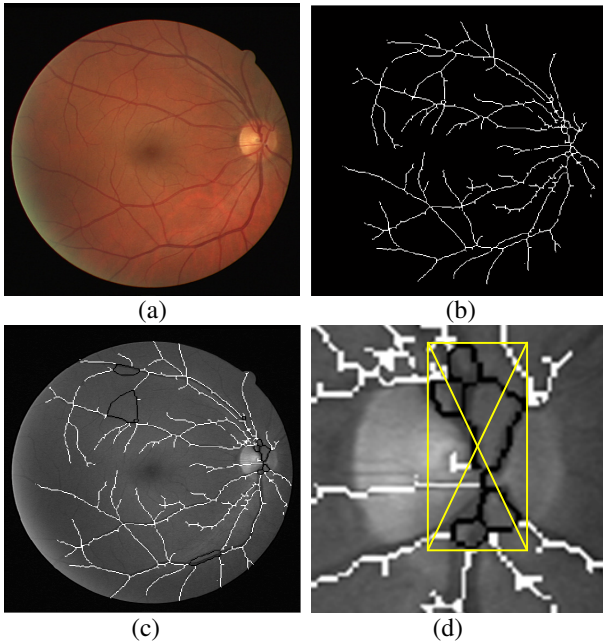


Figure 1. Construction of the method of most vasculature loops for OD localisation, (a) original colour image, (b) skeleton of the vasculature, (c) vasculature loops on the original gray image (white = branches, black = loops), and (d) Zoomed area of most loops with a boundary box.

OD centre is determined as the centre of the OD boundary. Figure 2 shows results from the proposed method to detect the boundary and final OD centre.

2.2. Fovea Localisation

The proposed method for the fovea localisation is based on defining a candidate ROI with reference to the established retinal landmarks, followed by a shape and intensity search. The two main retinal vessels (known as the arcade) can together be approximated as a parabola and in most retinal images the fovea is located within this arcade. After the vasculature detection, using the method described in an earlier paper [12], we followed the method described in [7] to fit the two main vessels as a parabola.

A parabolic Hough Transform is applied to the segmented thick vasculature to approximate the two main vessels into a parabolic curve, thus finding the vertex where the two main vessels emerge. As the OD centre is assumed to lie exactly where the vasculature emerges, the detected vertex of the parabola can be used as the initial estimate of the OD centre. On the basis of this parabola information, the candidate region for the fovea is defined as a circle with a diameter of twice the diameter of the OD (DD) along the main axis of the fitted parabola and centered at a distance of 2.5DD from the vertex. Although the fovea is equal in size to the OD [3], we select the ROI four times as large to ensure that all fovea pixels are within the selected ROI. The threshold value is calculated within the ROI in such a way

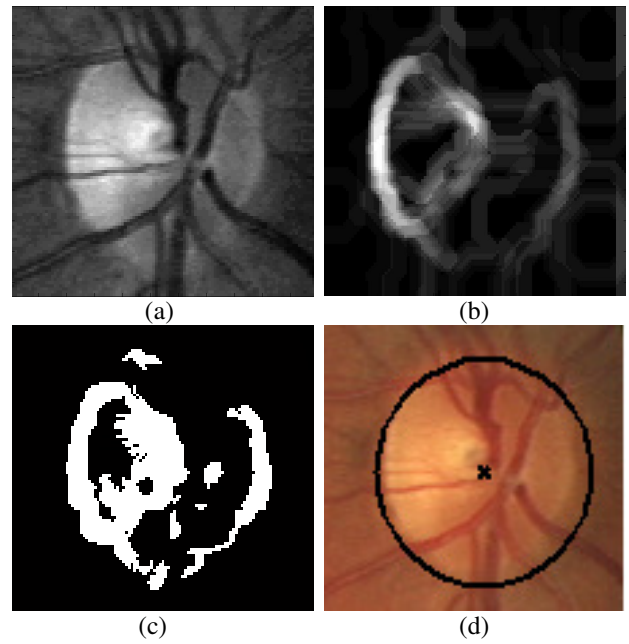


Figure 2. Steps of the method of most vasculature loops, (a) sub-image as ROI from initial OD centre, (b) ROI after applying gradient magnitude, (c) thresholding result, and (d) determined boundary and centre of the OD.

that the segmented area has an area not bigger than that of the OD. A scheme for fovea ROI overlaid on the original retinal image is illustrated in Figure 3.

Because the fovea is not completely obvious in some images, the lowest mean intensity is compared with the second lowest mean intensity to avoid mistaking the peripheral area where the illumination is relatively dark as in the fovea. The centroid of the lowest mean intensity cluster is specified as the center of the fovea when the difference is obvious and the number of pixels in the cluster is greater than 1/6 the area of the OD.

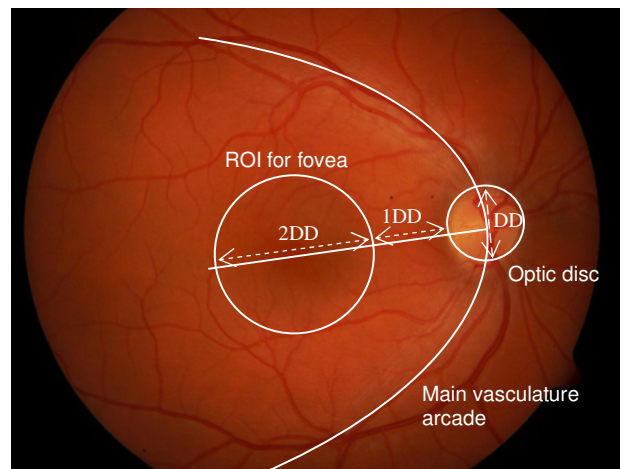


Figure 3. Geometric relations between the fovea and other retinal features, overlaid on an original image.

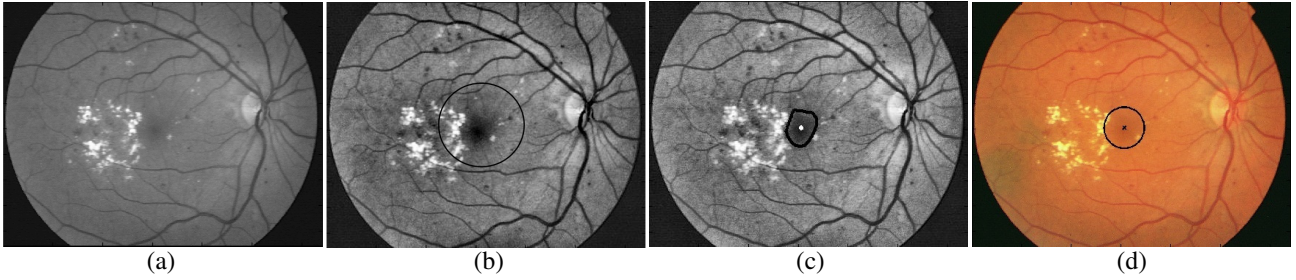


Figure 4. Steps of proposed method for the fovea localisation, (a) green channel image, (b) pre-processed image indicating the ROI for fovea localisation, (c) localised boundary and centre of the fovea taken from the binary result and illustrated on the pre-processed image, and (d) localised fovea after modification to a circle overlaid on the original image.

In the case of obscured fovea features due to lighting or being covered by lesions, the method may fail in finding a suitable threshold value. In such a case the fovea is approximated as a circle of diameter DD at the centre of the ROI. Figure 4 illustrates results of the fovea localisation, where the diameter of the modified circle is derived from the major axis length of the foveal boundary.

3. RESULTS AND DISCUSSION

The proposed method of OD localisation was trained and tested using a set of 138 retinal images (40 images from Drive dataset [14], 81 images from Stare dataset [15], and 17 images from Messidor Dataset [16]). These datasets include healthy images and pathological images with different types of abnormalities. This set was divided randomly into a training set of 40 images and test set of 98 images from all used datasets. Performance of the OD localisation was evaluated in comparison with an expert. In this technique the OD is correctly detected for all images except one from the Stare dataset. The success rate of OD localisation with the Messidor and the Drive datasets was 100%, whereas with the Stare dataset it was 98.8%.

Criteria of OD detection are used to evaluate the OD detection method by calculating its success rate and then classifying it as either successful or failed. The accuracy of OD centre and boundary localisation in a pixel basis is also important for accurate evaluation. But, due to the lack of any ground truth for OD localisation, we are unable to calculate the accuracy on a pixel basis. However, the success of the OD localisation was evaluated with regard to an expert. The performance of the proposed method was

Table 1. Comparison of OD localisation performances between the proposed method and previous related works.

Reference	Success rate% (Drive)	Success rate% (Stare)
Lalonde <i>et al.</i> [4]	--	71.6
Reza <i>et al.</i> [5]	95	95
Foracchia & Grisan [6]	--	97.6
Ying <i>et al.</i> [17]	97.5	--
Sekhar <i>et al.</i> [7]	100	98.8
Proposed Method	100	98.8

compared with previous related works using the Drive and Stare datasets as shown in Table 1.

The proposed fovea localisation method were trained and tested using a set of 268 retinal images (40 images from Drive dataset, 81 images from Stare dataset, 17 from Messidor dataset and 130 images from DIARETDB0 dataset [18]). These images represent both healthy and abnormal retinas with different types of abnormalities. This set was divided into a training set of 100 images (a mixture from both Stare and DIARETDB0) and a test set of 168 images from all datasets. Testing images were used with no attempt made to exclude images of poor quality or bad fovea appearance. The position of the fovea was identified by an experienced clinician as the ground truth. The proposed method has been evaluated with reference to the ground truth and found to achieve an overall success rate of 100% with the Drive dataset and 96.3% with the Stare dataset.

Fovea detection accuracy was measured in our work by calculating the Euclidean distance between fovea centres of the method result and the ground truth. The accepted distance for successful fovea localisation is adjusted to be proportional to the image size where the sensitivity of acceptance level can be changed and decided based on consultation with the clinicians and based on medical requirements. In accuracy calculations we used a distance of 30 pixels as a maximum tolerance for successful localisation in an image size of 640×480 pixels.

Because it is difficult to find methods tested by same criteria and same publicly available dataset, we implemented and tested some methods using the same criteria and dataset of our proposed method to compare with. A comparison between the success rate of the proposed method and some other previous related works tested on 40 images from the Drive dataset and 80 images from the DIARETDB0 dataset is presented in Table 2.

The intent behind selecting these two datasets is to demonstrate that accuracy result on normal and good quality images is higher than that of pathological and low quality images. As most Drive images are normal and good quality, most tested methods are found to achieve an average success rate of around 100%, while in the DIARETDB0, which has 110 pathological images, the average success rate is lower than that of the Drive dataset.

Table 2. Comparison of fovea localisation performances between the proposed method and previous related works.

Reference	Success rate% (Drive)	Success rate% (DIARETDB0)
Sekhar <i>et al.</i> [7]	100	95
Fleming <i>et al.</i> [8]	97.5	92.3
Sinthanay <i>et al.</i> [9]	95	93.8
Welfer <i>et al.</i> [10]	97.5	93.5
Tobin <i>et al.</i> [11]	100	95
Proposed method	100	96.3

4. CONCLUSIONS

In this paper, a computer-assisted retinal image processing system for the OD and fovea localisation is proposed. For OD localisation, we exploited the vasculature features inside the OD, where the most vasculature loops are allocated to be used for determining initial OD centre followed by applying morphological gradient on a ROI to determine the OD boundary and then the final OD centre. The fovea features along with its geometric relations with the vasculature and OD are used to determine boundary and centre of the fovea.

In both proposed methods we used heterogeneous images from different datasets in both training and testing operations. Thus our proposed method has been shown to be robust for different image types and quality levels. Also, we did not use parameters which may need setting for application to other images. In the proposed methods the vasculature features were used to guide the search for the OD and the fovea, thus they could be localised precisely even for images of low OD and fovea contrast, and the resulting accuracies of their localisation are superior to those methods that do not make use of the vasculature.

The performances of both methods are promising and could be developed further by validation with more datasets and their corresponding ground truths. This will contribute to further improvements, resulting in more robust retinal feature localisation that could be adapted for clinical purposes as part of an automated screening programme.

5. ACKNOWLEDGEMENTS

The authors would like to thank the Drive dataset centre [14], the Stare dataset centre [15], the Centre of Mines Paris Tech. [16], and the DIARETDB0 centre [18] for their co-operation in providing retinal images. Also they thank Dr T. Criddle from Liverpool Diabetic Eye Screening, Royal Liverpool University Hospital, UK for her medical consultation. A. K. Nandi would like to thank TEKES for their award of the Finland Distinguished Professorship.

6. REFERENCES

[1] J. Tang, S. Mohr, Y. D. Du, and T. S. Kern, "Non-uniform distribution of lesions and biochemical abnormalities within the retina of diabetic humans," *Curr. Eye Res.*, vol. 27, pp. 7-13, 2003.
 [2] M. D. Abramoff, M. Niemeijer, M. S. Suttorp-Schulten, M. A. Viergever, S. R. Russell, and B. van Ginneken, "Evaluation of a

system for automatic detection of diabetic retinopathy from color fundus photographs in a large population of patients with diabetes," *Diabetes Care*, vol. 31, pp. 193-8, 2008.

[3] "Grading diabetic retinopathy from stereoscopic color fundus photographs--an extension of the modified Airlie House classification. ETDRS report number 10. Early Treatment Diabetic Retinopathy Study Research Group," *Ophthalmology*, vol. 98, pp. 786-806, 1991.

[4] M. Lalonde, M. Beaulieu, and L. Gagnon, "Fast and robust optic disc detection using pyramidal decomposition and Hausdorff-based template matching," *IEEE Trans Med Imaging*, vol. 20, pp. 1193-2000, 2001.

[5] A. W. Reza, C. Eswaran, and K. Dimiyati, "Diagnosis of Diabetic Retinopathy: Automatic Extraction of Optic Disc and Exudates from Retinal Images using Marker-controlled Watershed Transformation," *J Med Syst*, vol. 29, 2010.

[6] M. Foracchia, E. Grisan, and A. Ruggeri, "Detection of optic disc in retinal images by means of a geometrical model of vessel structure," *IEEE Trans Med Imaging*, vol. 23, pp. 1189-95, 2004.

[7] S. Sekhar, F. E. Abd El-Samie, P. Yu, W. Al-Nuaimy, and A. K. Nandi, "Automated localization of retinal features," *Appl Opt*, vol. 50, pp. 3064-75, 2011.

[8] A. D. Fleming, K. A. Goatman, S. Philip, J. A. Olson, and P. F. Sharp, "Automatic detection of retinal anatomy to assist diabetic retinopathy screening," *Phys Med Biol*, vol. 52, pp. 331-45, 2007.

[9] C. Sinthanayothin, J. F. Boyce, H. L. Cook, and T. H. Williamson, "Automated localisation of the optic disc, fovea, and retinal blood vessels from digital colour fundus images," *Br. J. Ophthalmol.*, vol. 83, pp. 902-10, 1999.

[10] D. Welfer, J. Scharcanski, and D. R. Marinho, "Fovea center detection based on the retina anatomy and mathematical morphology," *Comput Methods Programs Biomed*, 2010.

[11] K. W. Tobin, E. Chaum, V. P. Govindasamy, and T. P. Karnowski, "Detection of anatomic structures in human retinal imagery," *IEEE Trans Med Imaging*, 26, pp. 1729-39, 2007.

[12] H. F. Jaafar, A. K. Nandi, and W. Al-Nuaimy, "Decision support system for the detection and grading of hard exudates from color fundus photographs," *J Biomed Opt*, vol. 16, pp.116001(1-10), 2011.

[13] Y. Qiao, and S. H. Ong, "Connectivity-based multiple-circle fitting," *Pattern Recognition*, vol. 37, pp. 755-765, 2004.

[14] J. Staal, M. D. Abramoff, M. Niemeijer, M. A. Viergever, and B. van Ginneken, "Ridge-based vessel segmentation in color images of the retina," *IEEE Trans Med Imaging*, vol. 23, pp. 501-9, 2004.

[15] The University of Clemson, "The STARE project," 2007, URL <http://www.ces.clemson.edu/~ahoover/stare/>

[16] T. Walter, J. C. Klein, P. Massin, and A. Erginay, "A contribution of image processing to the diagnosis of diabetic retinopathy--detection of exudates in color fundus images of the human retina," *IEEE Trans Med Imaging*, vol. 21, pp. 1236-43, 2002.

[17] H. Ying, M. Zhang, and J. C. Liu, "Fractal-based automatic localization and segmentation of optic disc in retinal images," *Conf Proc IEEE Eng Med Biol Soc*, vol. 27, pp. 4139-41, 2007.

[18] T. Kauppi, V. Kalesnykiene, J. K. Kamarainen, L. Lensu, I. Sorri, J. Pietila, H. Kalviainen and H. Unsitalo., "DIARETDB0: Evaluation database and morphology for diabetic retinopathy algorithm," *Technical report*, Lappeenranta University of Technology, Finland, 2006.